

## On the Behavior of Superpressure Balloons at 150 mb

NADAV LEVANON, ROBERT A. OEHLKERS, SCOTT D. ELLINGTON, WILLIAM J. MASSMAN  
AND VERNER E. SUOMI

*Space Science and Engineering Center, University of Wisconsin, Madison 53706*

(Manuscript received 3 October 1973, in revised form 6 February 1974)

### ABSTRACT

This paper presents measured data related to the question of how constant are "constant-level" balloons. The simultaneous use of two balloon-borne instruments, a radio altimeter and a pressure sensor, operating on entirely different principles, help to distinguish between sensor noise and true balloon altitude fluctuation. Four types of superpressure balloon altitude changes at the level of 150 mb were observed: (i) neutral buoyancy oscillations (NBO) with a period of about 200 sec and with peak-to-peak amplitude of up to 50 m, (ii) short-term oscillations with a period of  $\sim 1.2$  hr and peak-to-peak amplitudes of up to 80 m, (iii) diurnal half-cycle (day observations only) with an amplitude of up to 150 m, and (iv) possible trends of up to 120 m per day.

The data were obtained during four superpressure-balloon 150-mb flights in the Southern Hemisphere. These balloon flights were part of a test program for the TWERL Experiment. NCAR's GHOST balloons and navigation system were used, with the final version of the TWERLE radio altimeter and an early version of the pressure sensor.

The data are presented with a discussion of their limitations, mainly aliasing, ambiguity, and the absolute accuracy of the pressure sensor. A theoretical analysis of the NBO, with a spectrum analysis of supporting ground radar data, are given in the Appendix.

### 1. Introduction

Rare types of data were obtained during four superpressure balloon flights, launched from Ascension Island in July 1972. These flights were part of a test program for the Tropical Wind, Energy Conversion and Reference Level Experiment (TWERLE). The data are unique because they present, for the first time, simultaneous readings of pressure and altitude. Previous superpressure balloon flights included either a pressure sensor (Morel and Bandeen, 1973) or a radar altimeter (Heinsheimer *et al.*, 1972), but never both. In the large-scale TWERL Experiment the data will be collected by the Nimbus F satellite. Hence, data from each balloon will be read daily during one to three consecutive overpasses, each lasting less than 20 min. In the test program, NCAR's Global Horizontal Sounding Technique (Lally and Lichfield, 1969) was used where the balloon telemetry is transmitted at low rate, on the high-frequency band, to a network of ground stations. When conditions permitted, data from an entire day were obtained.

These two unique aspects of the data justify their presentation despite some sensor and telemetry limitations which are discussed in the next sections.

It should be pointed out that the raw data for these flights, and many other flights which did not include both sensors simultaneously, are tabulated in the

TWERLE Flight Test Program Data Summary, published by NCAR in December 1972.

### 2. Sensors and telemetry

This section includes a brief description of the sensors and the telemetry. It concentrates on an evaluation of their performance and the dependability of the data. It should be remembered that obtaining this evaluation was the main purpose of the test program. The resulting information on the behavior of the balloon was an additional bonus. It turned out to be very helpful toward optimizing such parameters as resolution, ambiguity, sampling rate and sampling coincidence. It is apparent that those parameters were far from optimum during the test program.

#### a. Radio altimeter

This sensor participated in the test program in its final version, and was the most reliable and accurate among the sensors. More than 40 such altimeters were flown prior to this test (Levanon, 1970; Stremmer *et al.*, 1972). Their absolute accuracy was checked against ground base radar, and their short-term accuracy against radiosonde constant rate of ascent. The altimeter absolute accuracy is specified at  $\pm 10$  m  $\pm 0.05\%$ , which at flight altitude of 15 km (150 mb) adds up to  $\pm 18$  m. Our many comparisons of radar altimeter data

against ground base radar, could not detect errors larger than within the specified range (Fig. 1).

The radio altimeter is basically a delay-lock pulse radar system. It is described in more detail elsewhere (Levanon, 1970; Stremler *et al.*, 1972). It is an absolute type of instrument whose accuracy depends mainly on the velocity of light. The output information appears as altitude-dependent frequency with the relation

$$h = \frac{c}{2} \left( \frac{n}{f} - \tau \right), \quad (1)$$

where  $c$  is the velocity of light,  $f$  the altitude-dependent output frequency,  $h$  the altitude,  $n$  the mode number, and  $\tau$  the internal delay. The data output frequency is also the repetition rate.

The mode number in (1) is the number of pulses (plus one) transmitted between the departure of a pulse and its return. In the TWERLE altitude range,  $n=3$  always. The only man-made parameter in the altitude measuring equation is  $\tau$ . It is set as 1.35  $\mu$ sec and it includes some internal delay and an estimate of the position of the peak of the waveform of the returned pulse. The  $\pm 10$  m specified error accounts for the possible shift in the peak position between rough and smooth ocean, and also includes the maximum temperature dependence of the internal delay. The  $\pm 0.05\%$  error is a result of the loop-locking fluctuations due to noise, assuming end-of-the-range signal strength, and a 1-sec averaging period. Altimeters flown on board ascending radiosondes indicated an rms deviation from a straight line of less than 0.02%.

*b. Pressure sensor*

The pressure sensor utilizes an aneroid capsule with capacitive coupling. The aneroid capacitor serves as the tuning capacitor of a Clapp oscillator. To minimize the effects of oscillator drift, the aneroid capacitor is compared to a reference capacitor, with a high quality relay switching between the two capacitors. The difference between the reference frequency and the aneroid frequency is the measure of pressure. The oscillator effect will be completely nullified if the two capacitors (or two frequencies) are equal. This was not the case in the early version of the pressure sensor which was used in the test program. A bias frequency difference of approximately 10% was maintained.

Temperature compensation was obtained by selection of reference capacitor and aneroid mount. The temperature dependence of the pressure sensor averaged over the range +25 to -25C is as follows:

Balloon identity	BLCP/UK	AP/KW	NARL/SD	AC/SG
$\Delta P/\Delta T$ [mb(°C) <sup>-1</sup> ]	+0.02	-0.003	-0.03	-0.05

The sensor temperature dependence deteriorated below -25C; it was also dependent on the rate of temperature change. The pressure sensor temperature was

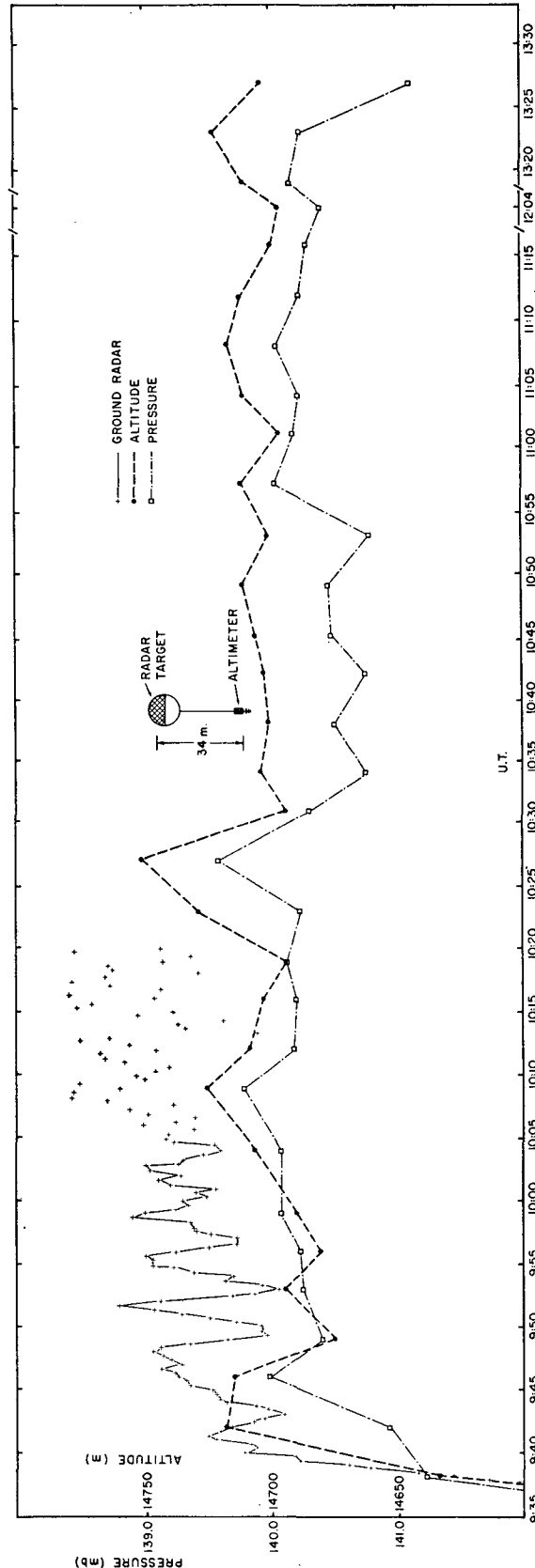


Fig. 1. Balloon-borne radio altimeter and pressure sensor data compared to ground radar observations from balloon AC/SG, launched from Ascension Island on 10 July 1972.

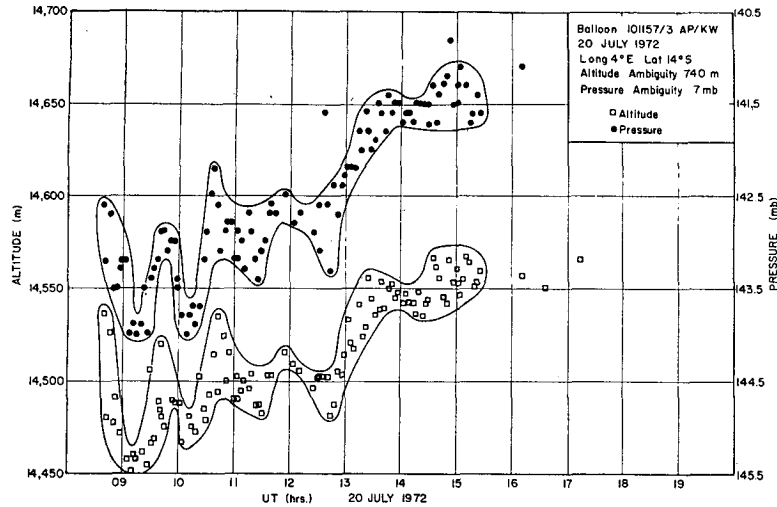


FIG. 2. Simultaneous readings of pressure and radar altitude from the second day of balloon AP/KW, launched 19 July 1972.

measured and telemetered to within an accuracy of  $\pm 2C$ . The sensor was placed in an 8-inch styrofoam sphere painted with white lead paint except for a 3-inch black strip on the equator. The temperature inside one such sphere is plotted on the data obtained for balloon AC/SG.

The pressure sensors were temperature-cycled and aged before calibration. Calibration was based on a Texas Instruments precision pressure gage Model 144. No calibration was performed at the launch site. Hence, periods of 2-4 weeks, including shipment from Wisconsin to Ascension Island, are not accounted for. Of the four pressure sensors, only the sensor used on balloon AC/SG was not allowed to adapt back to surface pressure, between calibration at 150 mb and arrival at flight ceiling (also 150 mb). This was done by placing

the sensor in a lexan bubble with a relief valve. The bubble was evacuated down to 200 mb immediately after calibration. The relief valve opened for the first time during the balloon ascent, at a pressure of 280 mb (10,300 m).

From the above discussion it is obvious that the pressure sensors used in the test program were unsatisfactory as far as absolute and long-term accuracy. The uncertainty in the absolute reading is estimated at  $\pm 3$  mb.

On the other hand, the short-term stability, for a period of a few hours around local noon, is estimated at better than  $\pm 0.2$  mb. This good short-term stability does not exist during sunrise and sunset, when large and fast temperature changes occur inside the sensor.

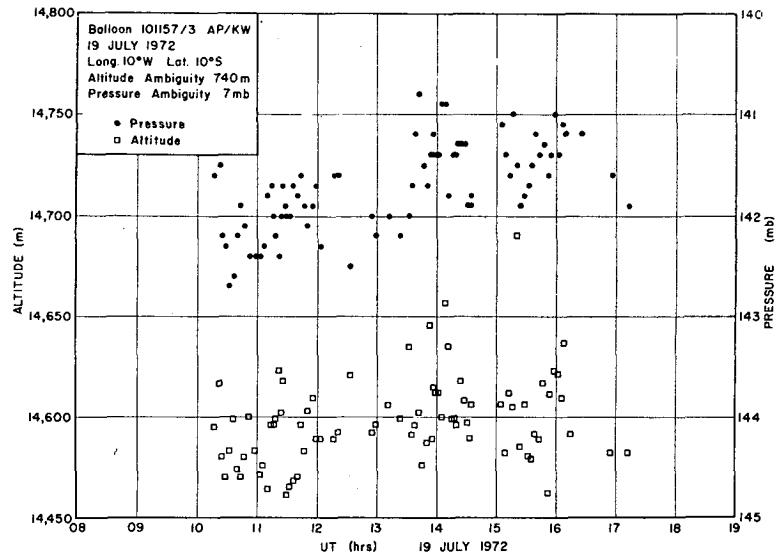


FIG. 3. Data from the 1st day of balloon AP/KW.

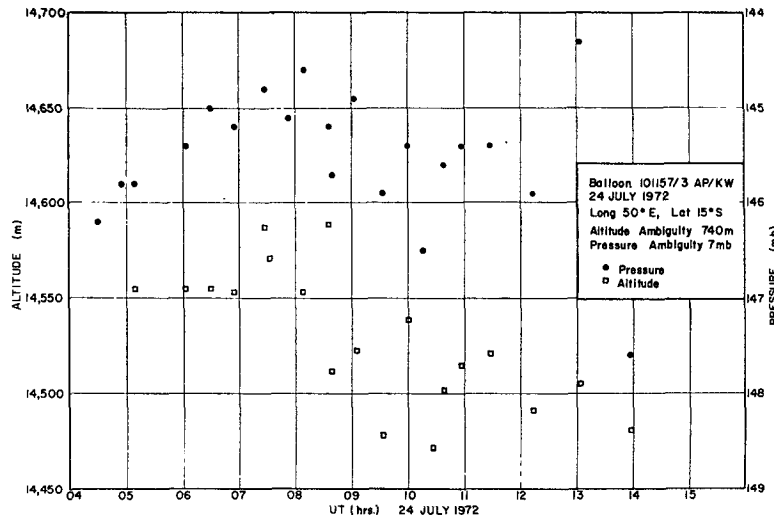


FIG. 4. Data from the 6th day of balloon AP/KW.

The pressure data for all the balloons were plotted without temperature correction. In the case of balloon AC/SG, where the pressure sensor was the most sensitive to temperature, a plot of the temperature of the pressure sensor was added.

*c. Telemetry*

The telemetry system used in the test program was identical to NCAR's Digi-GHOST. With regard to the two sensors discussed, the Digi-GHOST system performs sampling of the sensors' output frequency in a sequence, counting the frequency, storing it in a shift register, and finally modulating the coded information

on the 15-MHz transmitter. In the pressure sensor case both count-up and count-down are utilized to obtain the difference between the reference capacitor frequency and the aneroid capacitor frequency.

The telemetry system has 512 resolution elements per sensor. This determines the relation between the ambiguity and the resolution. In the pressure sensor case, typical resolution was 0.02 mb, resulting an ambiguity of approximately 10 mb. Typical resolution of the altimeter was 1.45 m, resulting an ambiguity of 740 m.

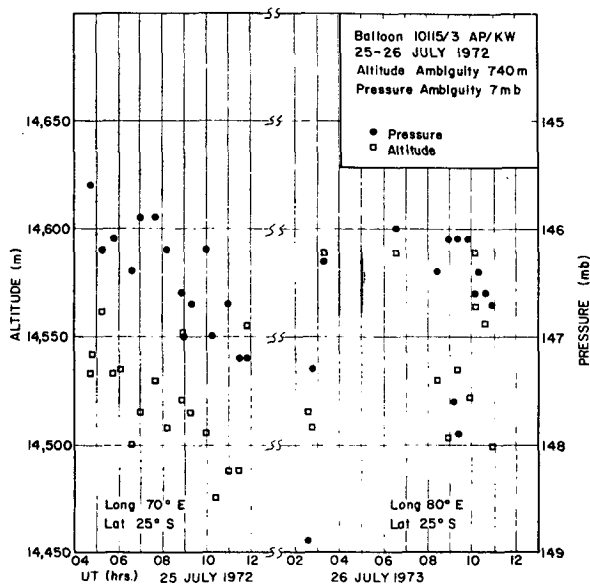


FIG. 5. Data from the 7th and 8th days of balloon AP/KW.

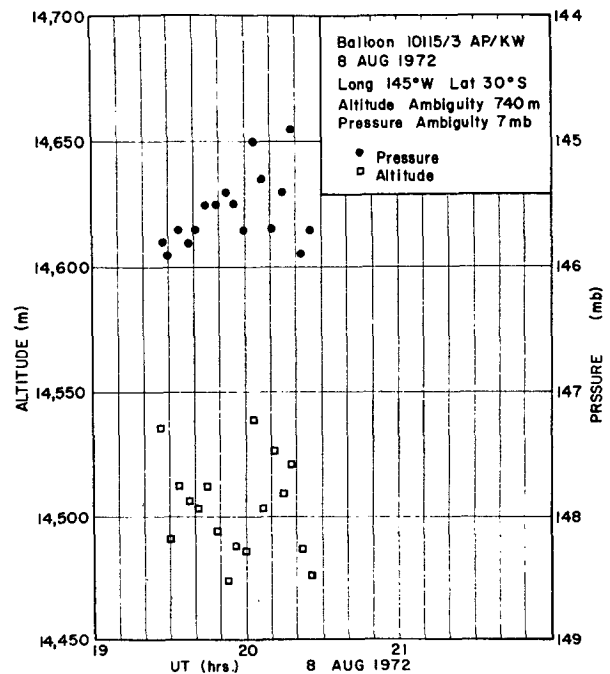


FIG. 6. Data from the 21st day of balloon AP/KW.

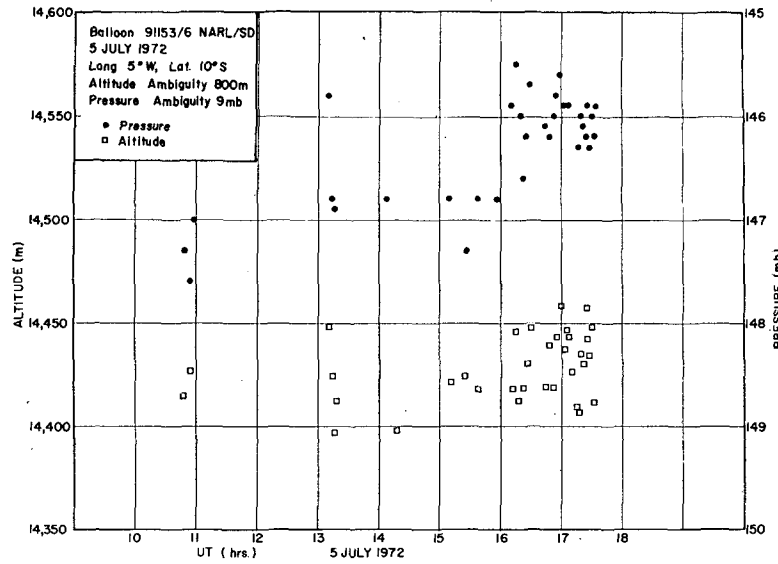


FIG. 7. Data from the 1st day of balloon NARL/SD.

A complete sequence of sampling and transmitting all the sensors data lasted 3.65 min, which is therefore the sampling rate for each sensor. The pressure reading was taken a minute later than the altimeter reading.

After the data from the test program were analyzed it became obvious that all four parameters were poorly chosen. As could be seen from the ground radar data in Figs. 1 and 18–23, the balloon altitude in these cases oscillated with the NBO period ~200 sec with a peak-to-peak altitude difference of ~50 m. The 3.65-min sampling rate of altitude will not show the NBO because of aliasing. Furthermore, the 1-min spacing between the altitude and pressure reading can result in

an error in determining the altitude of a specific pressure. This error will have a zero mean but a standard deviation close to the amplitude of the altitude fluctuation, e.g., 25 m in the case demonstrated in Fig. 1.

With the aliasing and coincidence problem, a resolution of 1.5 m and the comparable 0.02 mb, were clearly overspecified. On the other hand, the resulting ambiguity proved to be underspecified. Except for the first few days after launch, the ambiguity could not be resolved based on TWERLE data alone.

### 3. Pressure and altitude data

With the data limitation in mind, it seemed most reasonable to present the data in a form that will emphasize trends lasting between  $\frac{1}{2}$  hr and 1 day. This led to the vertical and horizontal scales as shown starting with Fig. 2. A ratio of 50 m for each 1 mb was chosen for convenience, although 44 m for each 1 mb would have agreed more with the hydrostatic equation. The pressure and altitude scales were aligned separately for each figure, so that the pressure data were offset slightly above the altitude data for clarity.

Each figure includes the following data: balloon number and telemetry identity letters, date of the data, longitude and latitude as calculated from the sun angle sensor, and the approximate ambiguity of the two sensors at the specified day. Fig. 2 represents the second day in the life of balloon AP/KW (launched 19 July 1972). In this figure the data from each sensor were enveloped to emphasize longer period trends, which could be resolved from the available sampling rate without aliasing. It should be repeated here that the pressure sensor on board balloon AP/KW was the least temperature-dependent [ $<0.01 \text{ mb } (^\circ\text{C})^{-1}$ ]; hence, the pressure data appears as telemetered, without tem-

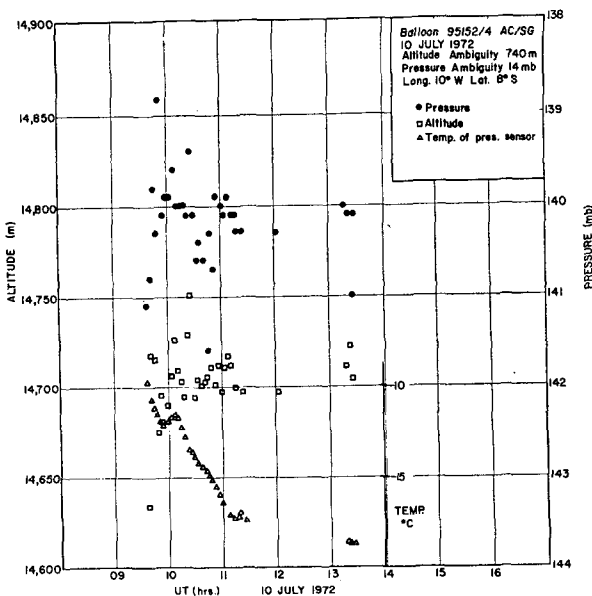


FIG. 8. Data from the 1st day of balloon AC/SG.

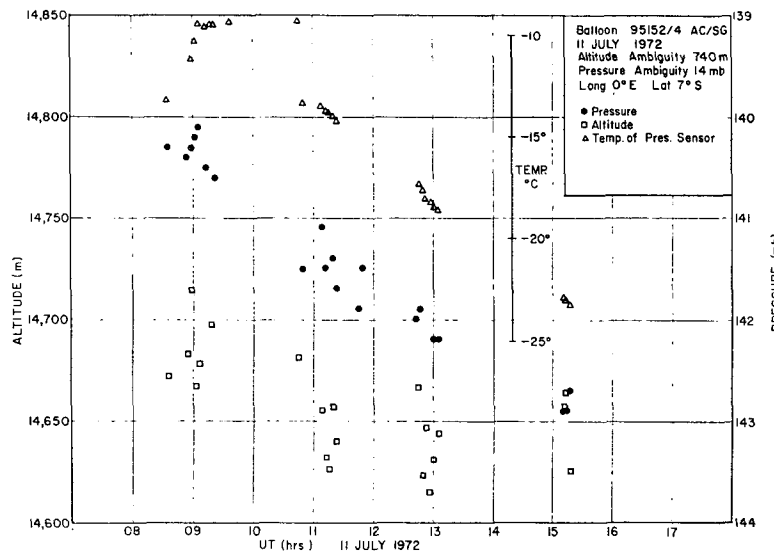


FIG. 9. Data from the 2nd day of balloon AC/SG.

perature correction. Several conclusions could be derived by inspecting Fig. 2.

1) Short-term trends, such as altitude oscillations with a period of  $\sim 1.2$  hr, appear in both sensors, with excellent correlations.

2) The thicknesses of the two envelopes are very well matched, indicating that the thickness is not the result of sensor noise, but of the NBO altitude fluctuations. This is supported by the ground radar tracking (Figs. 1 and 18-23). It is assumed that the telemetry contribution to noise is negligible. In general, one would expect the altimeter data to be slightly noisier than the pressure data since the ocean surface is an additional participant.

3) The poor correlation between individual altitude and pressure readings indicate that the 1-min spacing

between reading the two sensors is a significant part of the period of the NBO balloon altitude fluctuations. This is also supported by the ground radar tracking.

4) Finally, the entire-day trend toward higher altitude is emphasized more in the pressure than in the altitude data. This could be a result of several reasons: (i) an excessive pressure-scale expansion ( $50 \text{ m mb}^{-1}$  instead of  $44 \text{ m mb}^{-1}$  as derived from the hydrostatic equation); (ii) adaptation of the pressure sensor (this was only the second day of flight, after storage for almost one month at surface pressure); and (iii) true change in the altitude of the pressure surface.

Figs. 3-6 include the remaining available data from balloon AP/KW. The holes in the data are results of either being out of range from any of the ground station, or flying over land where the altimeter data de-

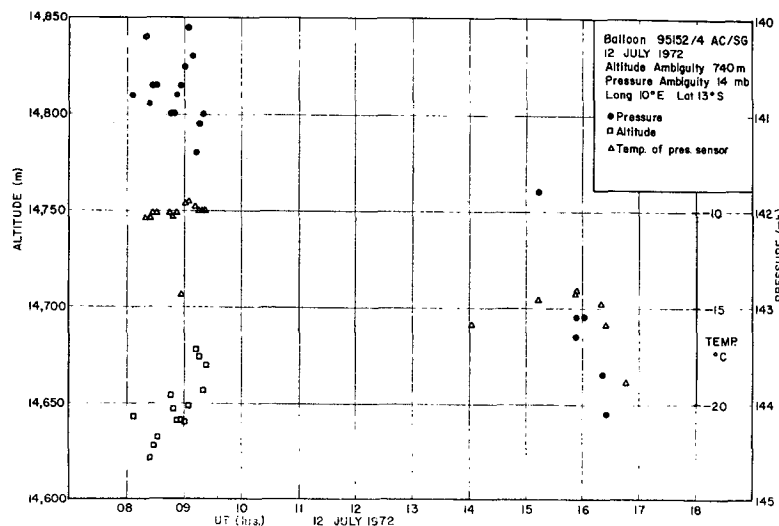


FIG. 10. Data from the 3rd day of balloon AC/SG.

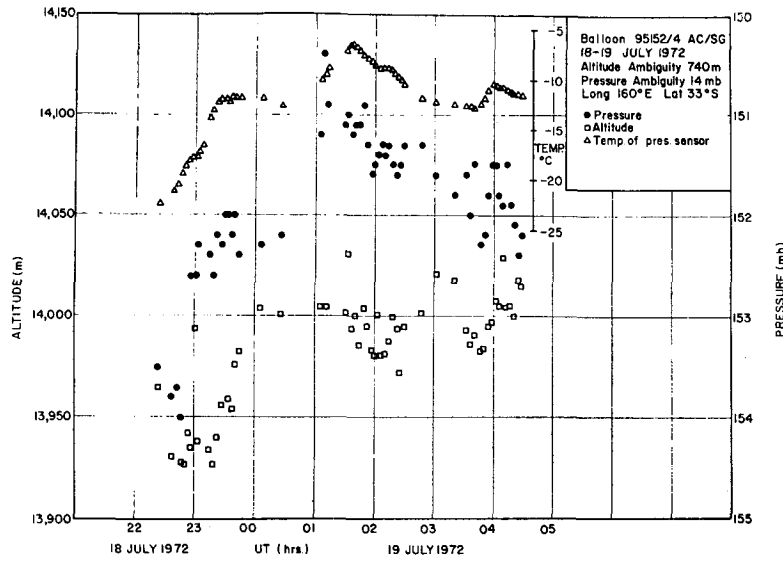


FIG. 11. Data from the 9th day of balloon AC/SG.

pend more on the terrain than on the balloon altitude changes. Balloon AP/KW remained flying till 31 August 1972, although the last day of meaningful altitude data was 8 August 1972.

Only the first day (5 July 1972) of balloon NARL/SD contained a reasonable amount of data (Fig. 7). The telemetry system on that balloon became erratic soon afterward.

Considerably more data were obtained from balloon AC/SG. This balloon had the most temperature-sensi-

tive pressure sensor. For this reason the temperature of the pressure sensor is plotted against the raw pressure data. Balloon AC/SG was launched on 10 July 1972 (Fig. 8 and Fig. 1). The second and third flight days appear in Figs. 9 and 10, respectively. Around noon on 12 July 1972, the balloon crossed the African Coast, which is why no altitude data are plotted for the afternoon. Fig. 11 includes the temperature increase due to sunrise (2200–2300 GMT 18 July). It is believed that the pressure readings during this period are too

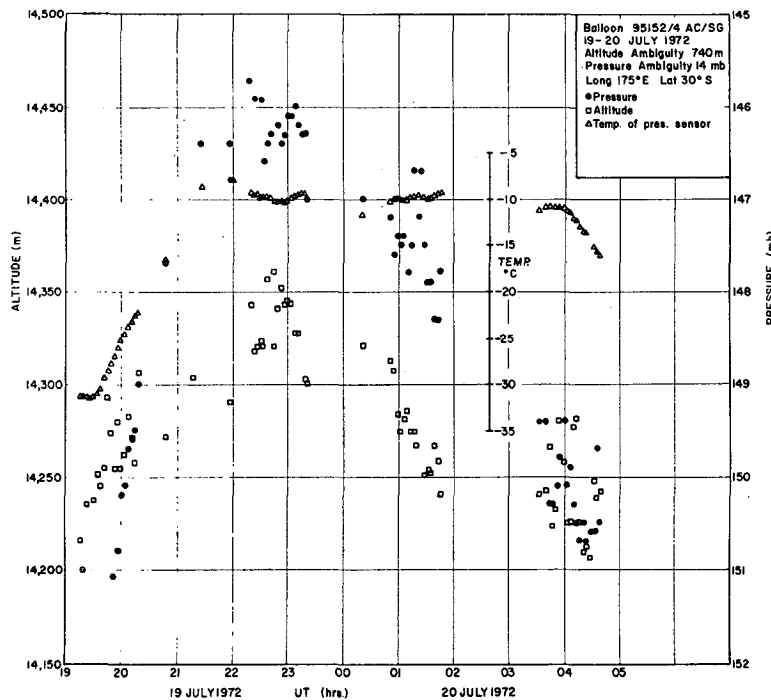


FIG. 12. Data from the 10th day of balloon AC/SG.

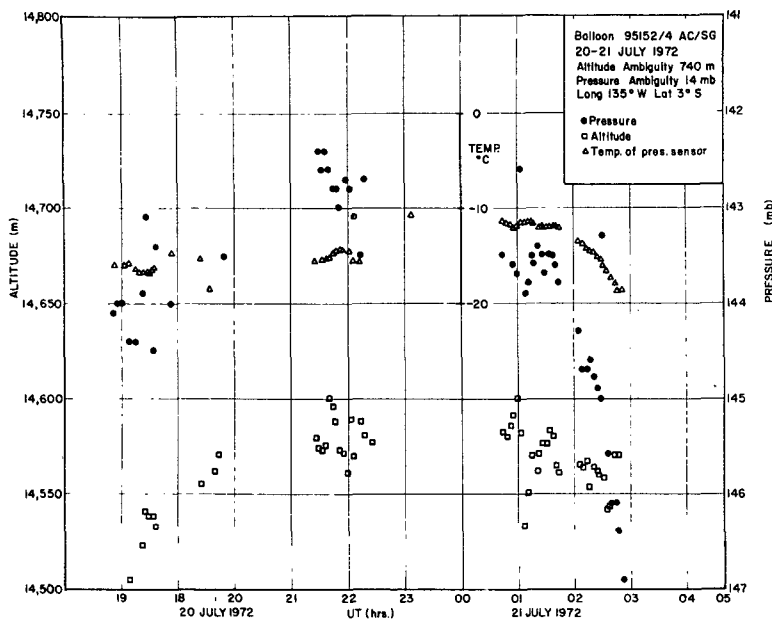


FIG. 13. Data from the 11th day of balloon AC/SG.

high. The same should apply to the sunrise and sunset periods of 19–20 July 1972 (Fig. 12). The behavior of balloon AC/SG on 19–20 July is typified by a strong diurnal half-cycle (day only). Using the altimeter readings, the balloon climbed 150 m from morning till noon, and dropped the same height from noon till evening. This agrees with observations by Morel and Bandeen (1973). Part of the rapid pressure increase during sunset, 0200–0300 GMT 20–21 July (Fig. 13), is also attributed to the rapid temperature drop inside the pressure sensor. The last two days of data from balloon AC/SG are given in Fig. 14. The diurnal cycle seems to be more emphasized in AC/SG than in any of the other

three balloons. Two other peculiarities of AC/SG were observed, and may be correlated to the large diurnal cycle:

1) AC/SG had overshoot its calculated flight altitude by 135 m, while BLCPUK, AP/KW and NARL/SD overshoot their altitudes by 15 m, 75 m and 75 m, respectively.

2) The NBO amplitude and period were slightly larger than the others (see the Appendix for comparison between AC/SG and AP/KW). On the other hand, it should be noted that day 19–20 July 1972 of balloon AC/SG included the longest daytime data recording period of all the balloons.

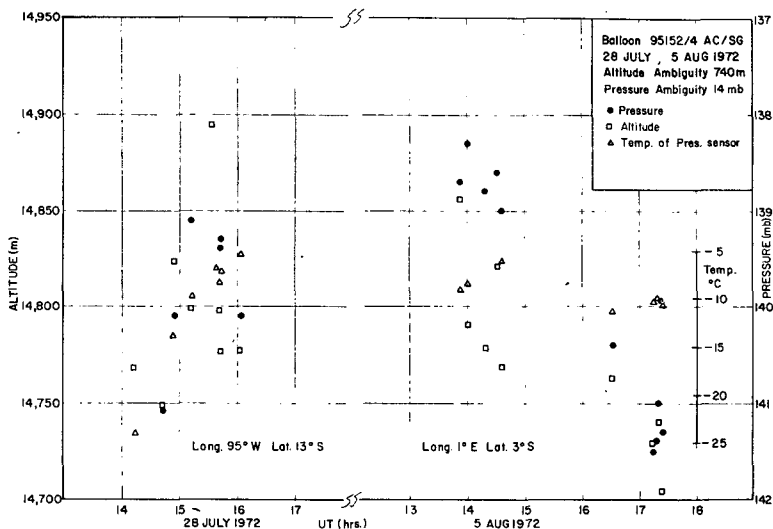


FIG. 14. Data from the 19th and 27th days of balloon AC/SG.



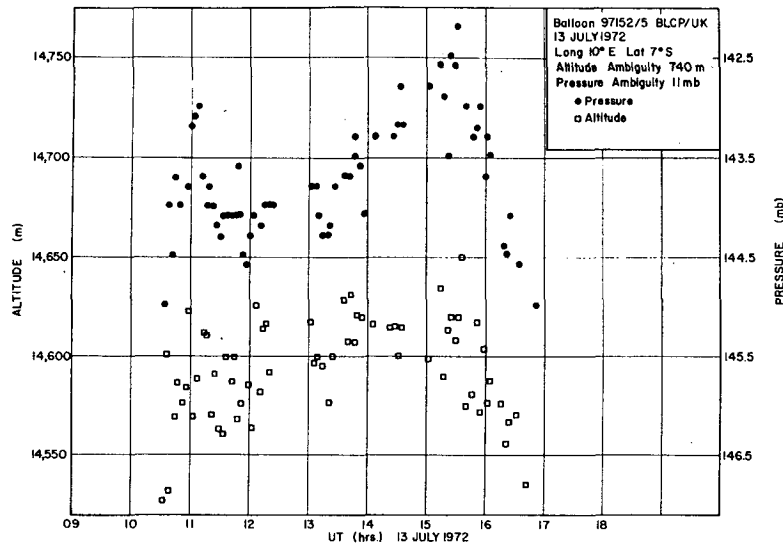


FIG. 15. Data from the 1st day of balloon BLCP/UK.

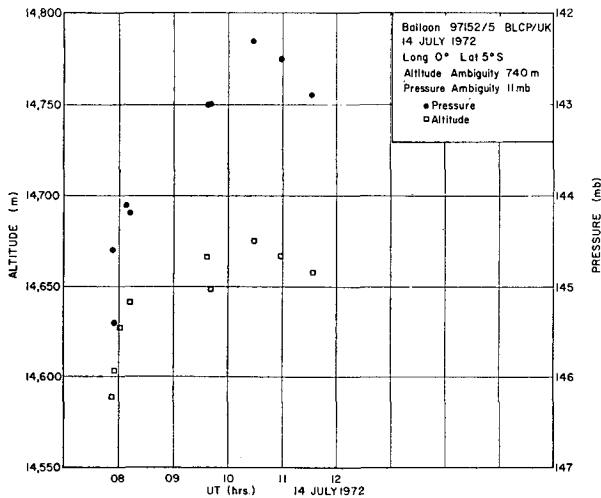


FIG. 16. Data from the 2nd day of balloon AC/SG.

Balloon BLCP/UK was short-lived. It was launched on 13 July 1972 and was last heard from on 20 August 1972. The first day is given in Fig. 15 where, again, the data spread is compatible in the two sensors. Fig. 16 is the morning of the second flight day, and Fig. 17 includes the remaining data received from this balloon. It should be pointed out that several data points per day were received in between the days presented here. They were too few, however, to indicate any trend, and to warrant being included in a figure. Had the absolute accuracy of the pressure sensor been better, such points would still be useful for the purpose of reference surface.

#### 4. Conclusions

The measurements described in this paper contribute to our knowledge of the behavior of superpressure balloons. *A priori* knowledge of typical balloon be-

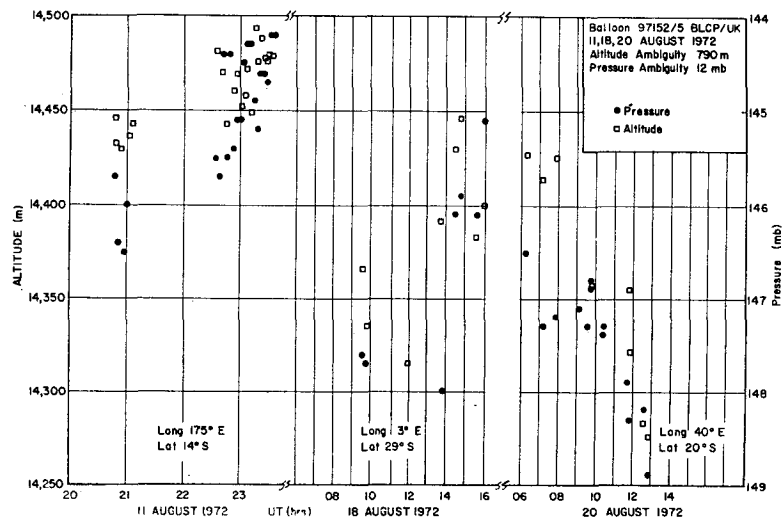


FIG. 17. Data from the 30th, 37th and 39th days of balloon BLCP/UK.

havior, and simultaneous altitude and pressure readings, will help to distinguish between balloon- and atmosphere-induced phenomena.

These data on balloon altitude and pressure fluctuations should also help in preparing specifications for future balloon sensors.

*Acknowledgements.* The work reported here has been supported by the National Science Foundation under Contract C660 and by the National Aeronautics and Space Administration under Contract S-70231-A.

The authors wish to acknowledge the contribution of the late Charles D. Blair III for his work on the altimeter development, and the late John A. Kruse for his work on the pressure sensor. Thanks are also due to B. Mozes of Meeda Ltd., Ramat-Gan, Israel, for his special efforts in the manufacturing of the radio altimeters. This work would not have been possible without the cooperation of V.E. Lally and E. W. Lichfield of the National Center for Atmospheric Research.

APPENDIX

**Superpressure Balloon Neutral Buoyancy Oscillations**

From the vertical equation of motion of a balloon (Hanna and Hoecker, 1971), it is possible to derive the period of neutral buoyancy oscillations (NBO). Assuming that the balloon drag acceleration and the atmospheric acceleration are negligible, then the restoring force is given by

$$M_b \frac{d^2Z}{dt^2} = (\rho_a V - M_b)g - \frac{1}{2} M_a \frac{d^2Z}{dt^2}, \tag{1}$$

where  $M_b$  is the mass of the balloon system (the balloon, the gas inside it, string, and payload),  $M_a$  the mass of atmosphere displaced by the balloon,  $\rho_a$  the

TABLE 1. Lapse rate versus NBO period.

$\gamma$ (°C km <sup>-1</sup> )	$\tau$ (sec)
0	188
.5	189
1.0	191
1.5	192
2.0	194
2.5	195
3.0	197
3.5	198
4.0	200
4.5	202
5.0	204
5.5	205
6.0	207
6.5	209
7.0	211
7.5	213
8.0	214
8.5	216
9.0	219
9.5	221
9.8	222

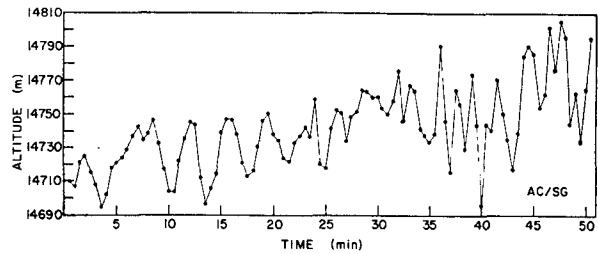


FIG. 18. Ground radar altitude data of balloon AC/SG after reaching flight altitude, on 10 July 1972.

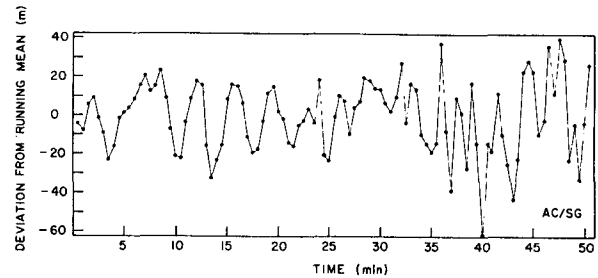


FIG. 20. The altitude data of Fig. 18 after removal of the constant drift.

density of the atmosphere,  $V$  the volume of the balloon, and  $g$  the acceleration of gravity. The term  $\frac{1}{2} M_a \frac{d^2Z}{dt^2}$  on the right-hand side of (1) is due to entrainment of part of the atmosphere by the balloon. For a spherical balloon near a static equilibrium level this has the equivalent effect of increasing the mass of the balloon system by 50% (Prandtl, 1952). Hence (1) reduces to

$$\frac{3}{2} M_b \frac{d^2Z}{dt^2} = (\rho_a V - M_b)g. \tag{2}$$

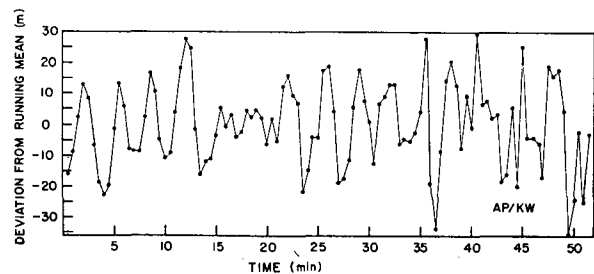


FIG. 21. The altitude data of Fig. 19 after removal of the constant drift.

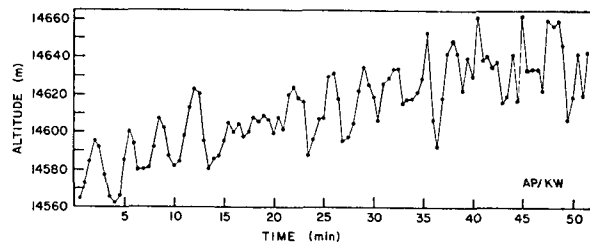


FIG. 19. Ground radar altitude data of balloon AP/KW after reaching flight altitude on 19 July 1972.

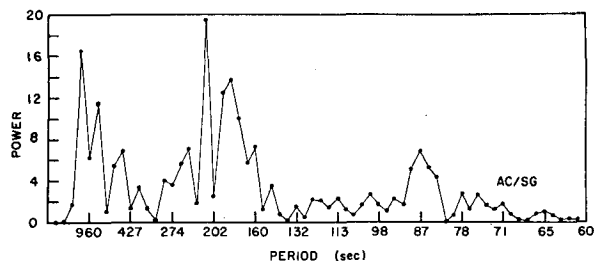


FIG. 22. Spectral analysis of the altitude fluctuations given in Fig. 20.

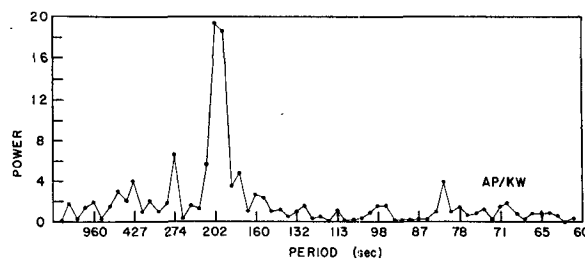


FIG. 23. Spectral analysis of the altitude fluctuations given in Fig. 21.

There are two factors that affect the balloon's NBO. As the balloon oscillates in the vertical, the density and pressure of the surrounding atmosphere change. The change in outside pressure causes a change in superpressure which in turn causes the balloon volume to expand or contract. Taking these into account, Eq. (2) can be rewritten to a very close approximation, as

$$\frac{d^2Z}{dt^2} = \frac{2}{3}g \left[ \frac{1}{\rho_0} \frac{\partial \rho_a}{\partial Z} (1 + K\Delta P) \right] (Z - Z_0), \quad (3)$$

$$K = + \frac{1}{V_0} \left( \frac{\partial V}{\partial P} \right)_T, \quad (4)$$

where  $Z_0$  is the static equilibrium height of the balloon,  $Z - Z_0$  the displacement from equilibrium,  $\rho_0$  the density of the atmosphere at equilibrium level,  $\Delta P$  the superpressure at equilibrium level,  $K$  the isothermal compressibility, and  $V_0$  the volume of the balloon at equilibrium level. Using the ideal gas law and the hydrostatic relation, it follows that

$$\frac{d^2Z}{dt^2} = - \left[ \frac{2}{3} \frac{g}{r} \left( \frac{g}{r} - \gamma \right) \left( \frac{1 + K\Delta P}{T_0} \right) \right] (Z - Z_0), \quad (5)$$

where  $r$  is the universal gas constant,  $T_0$  the atmospheric temperature at equilibrium level, and  $\gamma$  the environmental lapse rate. Since  $K\Delta P$  is very small compared to unity for superpressure balloons (Sommeria, 1970), the period  $\tau$  for the NBO is given approximately by

$$\tau = 2\pi \left[ \frac{3T_0(1 - K\Delta P)}{2g \left( \frac{g}{r} - \gamma \right)} \right]^{\frac{1}{2}}. \quad (6)$$

Table 1 gives this period in seconds for a range of lapse rates varying from isothermal to adiabatic. In computing Table 1,  $K\Delta P$  was estimated as 0.03 (Sommeria, 1970) and  $T_0$  as 206K.

From Table 1 one can see that the NBO period varies from 188 sec for an isothermal lapse rate, to 222 sec for an adiabatic lapse rate. This clearly shows that the

balloon NBO is not very sensitive to atmospheric conditions.

A spectral analysis was made using some of the radar data of balloons AP/KW and AC/SG taken at launch. Every 30 sec of data after the balloons had reached equilibrium level were used for the analysis. The raw altitude data are shown in Figs. 18 and 19 for balloons AC/SG and AP/KW, respectively. A linear regression removed the linear trend associated with the slow but constant balloon creep. Figs. 20 and 21 show this data for AC/SG and AP/KW, respectively, with the vertical axis being the height deviation from the linear regression. Figs. 22 and 23 show the result of the spectral analysis carried out on these data. The largest peaks in the power spectra correspond to the NBO. The peak is at about 210 sec for AC/SG and about 202 sec for AP/KW. The secondary peaks to the left of the NBO peak correspond to longer periods of oscillations and are probably due to atmospheric activity. Peaks to the right of the NBO peak are probably noise.

#### REFERENCES

- Hanna, S. R., and W. H. Hoecker, 1971: The response of constant-density balloons to sinusoidal variation of vertical wind speeds. *J. Appl. Meteor.*, **10**, 601-604.
- Heinsheimer, T. F., P. Trimm and J. P. Pommereau, 1972: The flight of ATMOS-1: An extended test of a balloon borne radar altimeter at the 100 mb level. Paper presented at 7th AFCRL Balloon Symp., 25-27 September 1972.
- Lally, V. E., and E. W. Lichfield, 1969: Summary of status and plans for the GHOST balloon project. *Bull. Amer. Meteor. Soc.*, **50**, 867-874.
- Levanon, N., 1970: Balloon borne radio altimeter. *IEEE Trans. Geosci. Elec.*, **8**, 19-30.
- Morel, P., and W. Bandeen, 1973: The EOLE experiment: Early results and current objectives. *Bull. Amer. Meteor. Soc.*, **54**, 298-306.
- Prandtl, L., 1952: *Essentials of Fluid Dynamics*. London, Blackie and Son Ltd., p. 342.
- Sommeria, G., 1970: Comparisons of the possibilities of measuring large-scale winds in the tropical troposphere using balloons and geostationary satellite photographs. Application to the EOLE-Pacific V experiment, the SE Pacific and the Amazon region, August-September 1969. Ph.D. thesis, University of Paris.
- Stremmer, F. G., N. Levanon and V. E. Suomi, 1972: A radio altimeter for balloon atmospheric sounding. *Preprints 2nd Symp. Meteor. Observ. Instr.*, 27-30 March 1972, San Diego, Amer. Meteor. Soc., 139-137.